

Grid Dependency Analysis for Performance Prediction of an Automotive Mixed Flow Turbine

Ahmed Ketata*, Zied Driss*

Laboratory of Electro-Mechanic Systems (LASEM), National School of Engineers of Sfax (ENIS), University of Sfax (US), B.P. 1173, Road Soukra km 3.5, 3038 Sfax, TUNISIA

*Corresponding author: ketata.ahmed.enib@gmail.com, zied.driss@enis.tn

Abstract The turbocharger which consists essentially on a radial turbine and a centrifugal compressor is commonly embedded to internal combustion engines in order to enhance its performance. The use of a mixed flow turbine instead of a radial one leads to better aerodynamic efficiency. The present investigation shows our optimized numerical model under steady conditions in purpose to predict the overall performance for an automotive vanned mixed flow turbine. Using the CFX 17.0 package, numerical results are obtained by solving the Reynolds averaged Navier Stokes equations by means of a finite volume discretization method. The standard k- ϵ turbulence model is used to close these equations. Based on the numerical solutions, the turbine performance and the reaction degree are computed. Equally, the distribution of the turbine output torque and its blades loading as a function of the isentropic velocity ratio are plotted. The mesh choice is based on the solution independency. Our numerical results show a good agreement compared to the test data.

Keywords: turbocharger, mixed flow turbine, performance, mass flow, Efficiency CFD, turbulence

Cite This Article: Ahmed Ketata, and Zied Driss, "Grid Dependency Analysis for Performance Prediction of an Automotive Mixed Flow Turbine." *American Journal of Energy Research*, vol. 5, no. 3 (2017): 97-102. doi: 10.12691/ajer-5-3-4.

1. Introduction

In order to respond to the environmental challenges, legislation was made to limit the emission of carbon dioxide from the exhaust of internal combustion engines. Manufacturers made small engines by means of downsizing technics. The employee of downsized engines yields to reduce its output power. Thus, adopting a boosting system which is based generally on the recovery of the exhaust gas energy becomes a necessity. Taking into account the installation constraints and the manufacturing cost, the turbocharger which presents a fundamental role in reducing engine fuel consumption is the best choice for automotive engine manufacturers. An automotive turbocharger consists mainly of a radial turbine and a centrifugal compressor. The turbochargers turbine recovers a part of the kinetic gas energy at the engine exhaust and converts it to a rotational energy at the compressor shaft. The global trend consists of enhancing the aerodynamic performance of the turbine and reducing occurring losses. A significant efficiency can be achieved at higher rotational speeds, but when regarding mechanical stresses, these operating conditions cannot be applied. Then, the turbocharger turbine should work with the maximum possible efficiency at lower rotational speeds. For thus, the radial turbine is commonly replaced by a mixed flow turbine in which the flow streamline have radial and axial components at the rotor inlet. Among earliest works that investigated on a mixed flow turbine is

that of Abidat [1]. This author designed and tested two highly loaded mixed flow turbines in the imperial college laboratory. His results show that both mixed flow rotors achieve the peak efficiency at lower optimum velocity ratios compared to the radial turbine. Furthermore, he confirmed that the turbine performance is heavily related to its rotor blade shape. In several anterior works, the turbine performance has been predicted using a mean line model seeing that provides an excellent performance prediction with a small calculation time and poor computational resources [2,3,4]. The average line model remains useful for industrial applications which require fastness to get solutions. However, it seems to be limited compared to the computational fluid dynamics (CFD) simulations. The work of Lymberopoulos et al. [5] performed earliest CFD simulations for a turbocharger turbine in which a quasi-three-dimensional solution based on the Euler equation was used. These authors observed that the flow proprieties variation in the circumferential volute exit particularly in the tongue region which is referred to a secondary stream. Hamel et al. [6] developed a CFD simulation, using the CFX package, for a mixed flow turbine under steady and pulsating conditions. They indicated the ability of the k- ϵ turbulence model and the frozen rotor approach to give a good prediction of the turbine performance and to capture the flow pattern inside the turbine passage. According to Padzillah [7], CFD simulation has succeeded to provide an excellent prediction of the aerodynamic performance of a nozzled mixed flow turbine under steady and pulsating conditions. Further, his work allowed obtaining several contours of

flow parameters such as the static pressure, the relative velocity and the absolute velocity for the turbocharger turbine at different defined locations. Roclawsk et al. [8] conducted CFD simulations for a mixed flow turbine under steady and unsteady conditions. Their results show that a lower degree of reaction yields to the improvement of the turbine isentropic efficiency at higher pressure ratios. Palfreyman and Martinez-Botas [9] launched a numerical simulation to capture the flow field within a single passage turbine rotor. They highlighted the advantage of the mixed flow turbine in which a smaller entropy generation in the zone near the tip surface suction was recorded compared to a radial turbine.

As a summary of the previous works, it is evident that most old works for turbocharger turbines are based on the turbine performance maps prediction by solving a one-dimensional code almost integrated with a mean line model. In view of the incapability of the average line model for giving a thorough analysis, CFD becomes popular and enables to understand with a detailed manner the flow behavior into such turbine in purpose to improve its efficiency. The following paper presents our optimized CFD model in order to predict the steady-state performance for a vanned mixed flow turbine. The turbine geometry modeling and the meshing methods are shown. Then, the turbine performance maps are computed by solving the RANS equations using the CFX solver and are compared to the test data. From this comparison, a grid independency analysis is made in order to validate our numerical models and to choose the optimal model. Several aerodynamic parameters such as the reaction degree, the blade loading, and the output torque are then commuted to more understand the effect of the operating point on the turbine performance for a fixed rotational speed.

2. Turbine Design

The mixed flow turbine becomes more used compared to the radial inflow turbine for automotive turbocharger applications. The mixed flow rotor is a combination of radial and axial configurations. Its design permits to obtain a non-zero inlet blade angle with maintaining of radial fiber elements rule. Thus, its design allows working efficiently at lower velocity ratios, to reduce inertia and then, to improve the turbocharger transient response. The automotive turbine investigated in this work consists mainly of a mixed flow rotor, a vane and a volute. The rotor is designed and tested firstly by Abidat [1]. The impeller blade shape is made with Polynomial Bezier curves giving different control points. The mixed flow turbine impeller consists of 12 blades with 40 mm of length. The inducer mean diameter of the turbine is 83.6 mm. However, its exducer hub diameter is 27 mm. The span height is fixed to be 18 mm at the inducer and 25.8 mm at the exducer. Its cone angle is 40° and its inlet blade angle is set to be 20° . However, it presents a variable exit flow angle keeping -52° as a mean value. The axial and radial tip clearances are fixed to 0.4 mm. The turbine inlet vane radius is 70 mm. The volute is a commercial twin entry vaneless one. Rajoo [10] modified this volute and he transformed it to acquire a nozzle ring conserving the

same area ratio distribution as a function of the azimuth angle. In this case, we are interested in the nozzleless configuration of the volute. Its centroid throat radius and its throat area are respectively about 100 mm and 3300 mm^2 . However, its tongue position is set to be 50° . Figure 1 shows the developed three-dimensional model of the full mixed flow turbine stage.

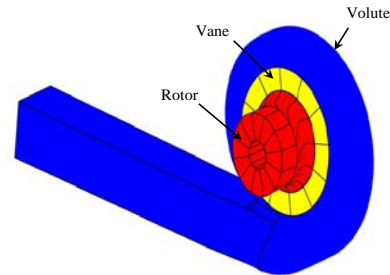


Figure 1. Computational domain

3. Numerical Method

Conducted simulations are based on Reynolds averaged Navier-Stokes equations of mass, momentum, and energy conservation for compressible flow. The commercial Ansys CFX 17.0 which is a CFD package including a finite volume method for the discretization is utilized to solve implicitly these equations with a pressure-based solver. The standard k- ϵ turbulence model is chosen to solve the additional terms which are due to the Reynolds decomposition. This turbulence model presented excellent capabilities to compute the flow in several anterior aerodynamic works [11,12,13]. The approach of the Multiple Reference Frame (MRF) with an automatic pitch is used to model the rotating domain. Good results are obtained with this method [14]. The choice of the boundary conditions is an essential step and requires a particular care for an exact definition of the reality. The revolution speed of the rotating domain is fixed to be 59783.4 rpm. A total pressure of 213996 Pa and a total temperature of 343 K are set at the turbine inlet boundary. However, an average static pressure instead of a static pressure is defined at the turbine exit to avoid the creation of the reverse flow during the computing process.

4. Grid Dependency

This section provides several meshing capabilities using the ICEM-CFD 17.0 software in purpose to better adjust our numerical model with the physical problem in question. The accuracy of the numerical results is related significantly to the mesh quality and size. In fact, the computational domain of the full turbine stage is divided into tetrahedral elements creating an unstructured meshing. The volute tongue, interfaces, and turbine blades are refined more than other regions using the local meshing parameter of the ICEM-CFD software. A gradual cell size transition was made for the zone separating between coarse and fine mesh regions. Furthermore, an inflation of ten prism layers is applied to the wall near zones by fixing the first cell high. This inflation is used to guarantee that

the non-dimensional wall distance still in the range required by the turbulence model. Three sizes of the meshing are generated by varying each time the cell size. The coarse meshing consists of 30287 cells and 9282 nodes when the medium meshing consists of 329619 cells and 106070 nodes. However, the fine meshing is composed by 1155129 cells and 2059178 nodes. Figure 2 presents the two-dimensional views from the z axis for the generated unstructured meshing. However, Figure 3 shows the three-dimensional views of the meshing for different sizes. To qualify the mesh size effect on the performance prediction accuracy, a comparison of the numerical results for each mesh size to the test data is made. For this comparison, the distribution of both the mass flow parameter (MFP) and the total to static isentropic efficiency are computed respectively as a function of the pressure ratio and the velocity ratio. Figure 4 presents the superposition of the distribution of these parameters gathered from our CFD simulations for each generated mesh and the experimental data collected by Romagnoli [15]. From Figure 4, a satisfactory agreement has been observed between the experimental and numerical results. Table 1 presents the standard deviations of both the isentropic efficiency and the mass flow parameter computed for different mesh sizes. For the coarse mesh, the standard deviations of the efficiency and the mass flow parameter are found to be respectively 11.50 % and 8.24 %. However, these deviations decrease significantly to be respectively 2.37 % and 4.69 % when the fine mesh is used. From these results, it has been observed that the numerical prediction of the isentropic efficiency is more sensitive to the mesh size than that of the mass flow rate. Besides, this deviation increases with the drop of the mesh size. Furthermore, this deviation stills in an acceptable range. Taking into account the limitations of our computational resources as well as the resolution time for the solution convergence, the medium mesh which consists of 329619 tetrahedral cells seems to be the best choice for predicting accurately the turbine performance.

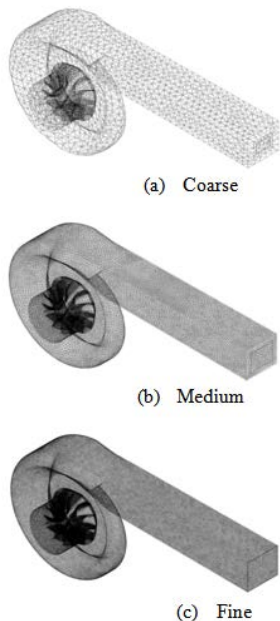


Figure 2. 3D views of the meshing

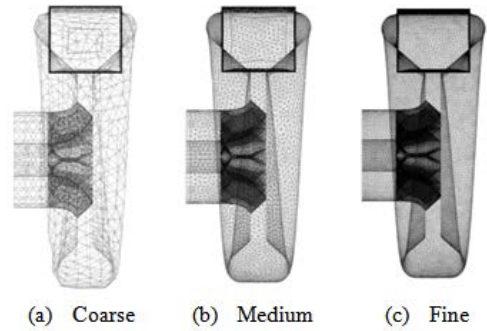


Figure 3. 2D views of the meshing

Table 1. Deviation from experiments.

Mesh	SD-Efficiency (%)	SD-MFP (%)
Coarse	11.50	8.24
Medium	2.37	4.69
Fine	2.51	6.70

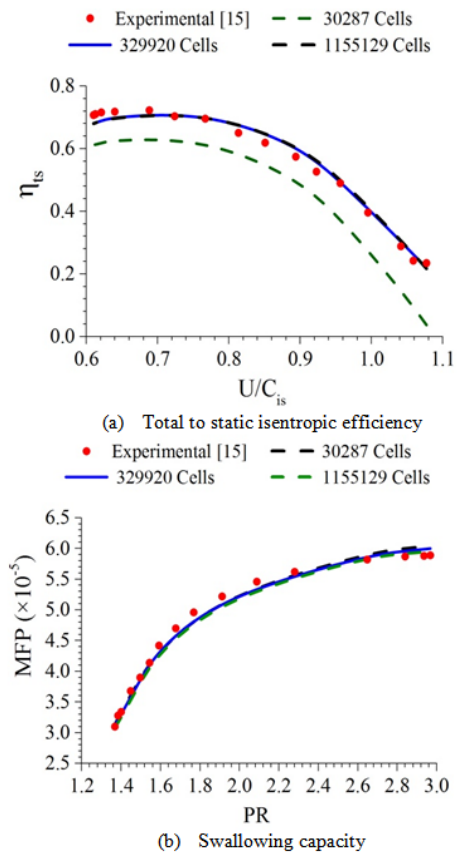


Figure 4. Comparison with experiments

5. Results and Discussion

5.1. Efficiency

Figure 5 shows the distribution of the total to total and the total to static isentropic efficiencies. The total to total and the total to static efficiencies present practically the same trend as a function of the isentropic velocity ratio excluding the zone defined by higher velocity ratios. According to these results, it can be seen that the total to total efficiency increases with a nonlinear manner as the velocity ratio drops. However, the total to static isentropic efficiency increases when the velocity ratio decreases until

it attains its peak value. From this point, it returns to drop. In fact, the gap between values of the total to total efficiency and the total to static efficiency remains nearly at the same level for a velocity ratio less than 0.7. For velocity ratios higher than 0.7, it can be seen that this gap increases and this fact is due mainly the significant rise of the kinetic energy at the rotor exit. Furthermore, it has been observed that the peak efficiency occurs at an optimum velocity ratio slightly less than 0.7 which presents typically the point of the peak efficiency for a radial inflow turbine. Then, the mixed flow turbine works efficiently at lower velocity ratios compared to the radial configuration.

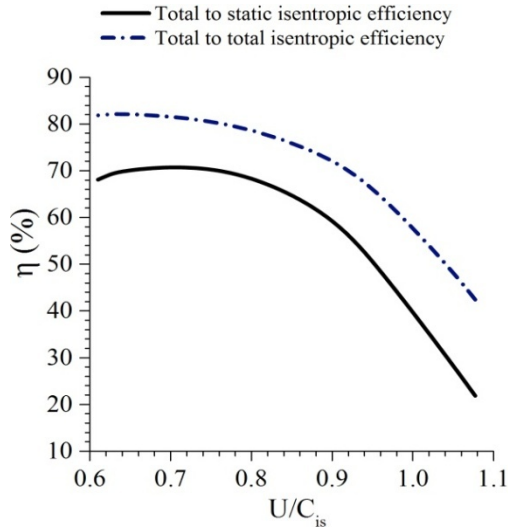


Figure 5. Efficiency Vs Velocity ratio

5.2. Mass Flow Rate

Figure 6 illustrates the evolution of the mass flow rate as a function of the pressure ratio. It has been noted that the mass flow rate increases, with a nonlinear trend, with the surge of the pressure ratio. At higher pressure ratios, the mass flow rate stills nearly in the same level. In these conditions, the mass flow rate becomes approximately insensitive to the change of the pressure ratio. This limitation of the mass flow rate is referred to the choked flow which is a characteristic of the sonic blockage. At this zone of the turbine maps, an aerodynamic loss which is due to the flow blockage. The value of the choking mass flow rate is about 0.69 and it is first recorded at 2.9 of the pressure ratio.

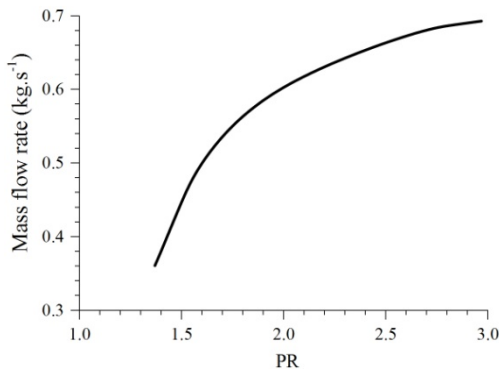


Figure 6. Mass flow rate Vs Pressure ratio

5.3. Reaction Degree

Figure 7 presents the distribution of the turbine degree of reaction as a function of the velocity ratio for different mesh sizes. From these results, it is obvious that the fine and medium mesh sizes give practically the same trend of the reaction degree distribution with close values. However, the prediction of the degree of reaction for the coarse mesh is found to be far to that obtained using higher cell numbers of the meshing. This fact confirms again our meshing choice discussed above.

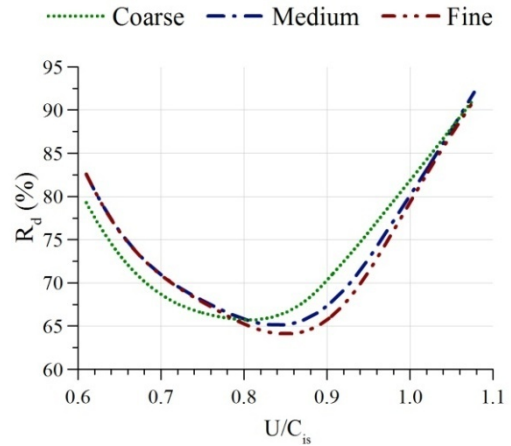


Figure 7. Degree of reaction Vs. Velocity ratio

5.4. Output Torque

Figure 8 shows the distribution of the torque available in the turbine shaft against the velocity ratio for different meshing sizes. On the one hand, it can be seen that the distribution of the torque gathered from the fine and medium sizes of the mesh are practically the same. However, values of the shaft torque obtained using the coarse mesh are considerably far to that found in the other mesh sizes especially at lower velocity ratios. On the other hand, from these results, it has been observed that the shaft torque is strongly sensitive to the variation of the velocity ratio. In fact, the shaft torque decreases gradually when the velocity ratio increases. Thus, higher torque is reached at higher pressure ratios. This fact is considerably related to the turbine blades loading.

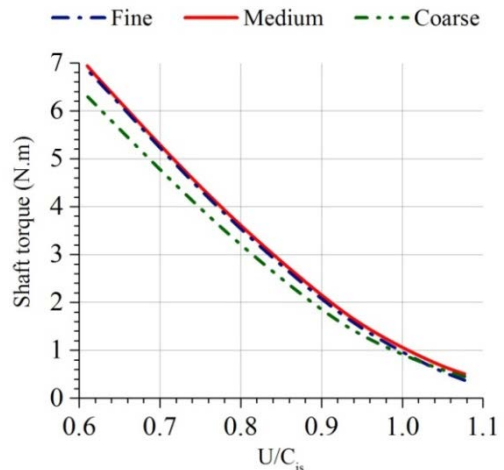


Figure 8. Output torque Vs. Velocity ratio

5.5. Blade Loading

Figure 9 presents the distribution of the static pressure normalized to the turbine inlet total pressure throughout the normalized streamwise at different pressure ratios for 0° of the circumferential position.

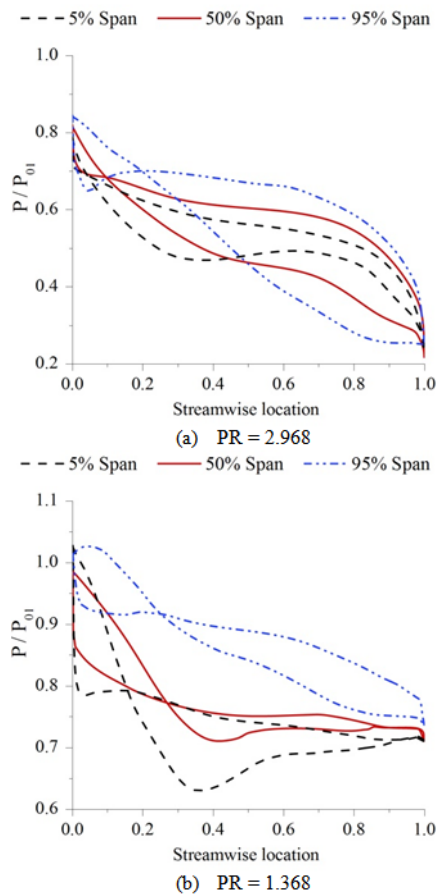


Figure 9. Blade loading at different pressure ratios

From these results, it has been observed that the turbine blade loading is greater for lower pressure ratios than higher pressure ratios. Thus, the static pressure at the blade surfaces increases with the decrease of the pressure ratio. Furthermore, the static pressure is found to be evidently higher at the shroud side than the hub side at a fixed value of the pressure ratio. Near the leading-edge zone, it has been noted that the suction surface presents higher static pressure than the pressure surface of the blade. This negative blade loading is more important for lower than higher expansion ratio. This fact can be explained by the change of the incidence angle across the span length of the leading edge as well as to the occurring secondary flow due to the tip blade leakage. This negative blade loading, especially at lower pressure ratios, is among the major causes of the decrease of the turbine shaft generated torque observed in the previous section.

6. Conclusions

In this paper, it has been noted that the numerical results of the efficiency are more sensitive to the mesh size than that of the mass flow rate. The good agreement

found between the numerical results and the test data confirms the validity of our numerical model. Based on the grid independency analysis, the unstructured mesh which consists of 329619 tetrahedral cells and 106070 nodes seems to be a satisfactory choice for the prediction of the turbine stage performance under various steady conditions. Results confirm that the mass flow rate increases substantially with the surge of the turbine expansion ratio and it becomes limited at the choking point. However, the peak efficiency occurs at an optimum velocity ratio less than 0.7. Furthermore, the reaction degree is considerably influenced by the variation of the isentropic velocity ratio. The same behavior has been observed for the available torque in the turbine shaft. A negative blade loading is recorded at the leading-edge, and it becomes more important at lower expansion ratios. This negative blade loading yields eventually to the decline of the turbine shaft torque at lower expansion ratios.

Nomenclature

MFP	mass flow parameter, $\text{kg}\cdot\text{s}^{-1}\cdot\text{K}^{0.5}\cdot\text{Pa}^{-1}$
P	pressure, Pa
PR	Pressure ratio, dimensionless
R_d	degree of reaction, dimensionless

Greeks

η	isentropic efficiency, dimensionless
--------	--------------------------------------

Abbreviations

CFD	computational fluid dynamics
MRF	multiple Reference Frame
3D	three-dimensional
2D	two-dimensional

Subscripts

ts	total to static
0	stagnation condition
1	turbine inlet

References

- [1] M. Abidat, Design and testing of a highly loaded mixed flow turbine. PhD thesis, Imperial College, London, 1991.
- [2] S. M. Futral, C. A. Wasserbauer, Off design performance prediction with experimental verification for a radial-inflow turbine, NASA TND-2621 (1965).
- [3] A. J. Glassmann, C. A. Wasserbauer, Fortran program for predicting off-design performance of radial inflow turbines, NASA TN-D-8063 (1975).
- [4] P. L. Meitner, A. J. Glassman, Computer code for off-design performance analysis of radial inflow turbines with rotor blade sweep, DTIC Document (1983).
- [5] N. Lymberopoulos, N. C. Baines, N. Watson, *Flow in single and twin entry radial turbine volutes*, ASME Gas Turbine and Aeroengine Congress paper 88-GT-59 (1988).
- [6] M. Hamel, M. Abidat, S.A. Litim, Investigation of the mixed flow turbine performance under inlet pulsating flow conditions, C. R. Mecanique 340 (2012) 165-176.
- [7] M. H. Padzillah, Experimental and numerical investigation of an automotive mixed flow turbocharger turbine under pulsating flow conditions. PhD thesis, Imperial College, London, 2014.
- [8] H. Roclawski, M. Gugau, F. Langecker, M. Böhle, *Influence of degree of reaction on turbine performance for pulsating flow conditions*, Proceedings of the ASME Turbo Expo (2014).
- [9] D. Palfreyman, and R. Martinez-Botas, *Numerical study of the internal flow field characteristics in mixed flow turbines*, Proc of ASME Turbo Expo GT2002-30372 (2002).

- [10] S. Rajoo, Steady and pulsating performance of a variable geometry mixed flow turbocharger turbine, PhD thesis, Imperial College, London, 2007.
- [11] S. Driss, Z. Driss, I. Kallel-Kammoun, Computational study and experimental validation of the heat ventilation in a living room with a solar patio system, *Energy and Buildings* 28 (2016) 40-119.
- [12] Z. Driss, O. Mlayeh, S. Driss, D. Driss, M. Maaloul, M.S. Abid, Study of the incidence angle effect on the aerodynamic structure characteristics of an incurved Savonius wind rotor placed in a wind tunnel, *Energy* 894 (2016) 908-113.
- [13] Z. Driss, O. Mlayeh, D. Driss, M. Maaloul, M.S. Abid, Numerical simulation and experimental validation of the turbulent flow around a small incurved Savonius wind rotor, *Energy* 74 (2014) 506-17.
- [14] J.W. Lam, Q. Roberts, G. McDonnel, *Flow modelling of a turbocharger turbine under pulsating flow*, Proceedings of IMechE International Conference on Turbochargers and Turbocharging (2002) 181-197.
- [15] A. Romagnoli, R.F. Martinez-Botas, *Performance prediction of a nozzled and nozzleless mixed-flow turbine in steady conditions*, *International Journal of Mechanical Science* 53 (2011) 557-574.